

Structural and Optical Properties of Al₂O₃ Nanostructures Prepared by Hot Water Treatment Method



Israa Abdullhasan Abbas^{ID}, Khalidah. H. Al-Mayalee*^{ID}

Department of Physics, Faculty of Education for Women, University of Kufa, Najaf 54001, Iraq

Corresponding Author Email: khalidah.almayali@uokufa.edu.iq

Copyright: ©2024 The authors. This article is published by IETA and is licensed under the CC BY 4.0 license (<http://creativecommons.org/licenses/by/4.0/>).

<https://doi.org/10.18280/rcma.340414>

ABSTRACT

Received: 24 June 2024
Revised: 9 August 2024
Accepted: 19 August 2024
Available online: 27 August 2024

Keywords:

Aluminum oxide (Al₂O₃), HWT method, nanostructures, high porosity, optical properties

Aluminum oxide (Al₂O₃) nanostructures were synthesized on an aluminum foil substrate by green synthesis method using the hot water treatment method at 75°C for 1, 7, 15, and 30 minutes. In this study, growth time was varied to study its effect on the Al₂O₃ nanostructure's size and density. The morphological and structural properties of the as-prepared Al₂O₃ nanostructures were investigated using SEM imaging and XRD analysis, and the optical properties were studied through UV-Vis spectroscopy. Scanning electron microscopy (SEM) investigations revealed porous agglomerated Al₂O₃ nanostructures, and the porous nanostructured particle size decreased in the 80 nm-35 nm range as the synthesis reaction time increased from 1 to 30 minutes. X-ray diffraction (XRD) analysis indicated the crystalline behavior increased with increasing time. The optical properties results showed that Al₂O₃ nanostructures display a relatively broad absorption spectrum across the ultraviolet region. Furthermore, the energy gap (E_g) increased from 3.44 to 3.78 eV when the immersion time increased from 1 minute to 30 minutes, respectively. These results have a significant impact on the Al₂O₃-assisted electronic application based on HWT Al₂O₃ nanostructures for a sustainable green earth.

1. INTRODUCTION

Nanostructured materials have been intensively researched during the last few decades due to their unique physical and chemical properties such as temperature stability, melting point, electrical and thermal conductivity, catalytic activity, light absorption, and wettability [1]. Nanostructures like nanowires, nanosheets, and nanoparticles provide immense technological advantages to be used in potential industrial and biomedical applications such as sensors, optical devices, catalysts, and drug delivery system [2]. The smaller size of metal oxide nanostructures (NSs) leads to high stability, high surface to volume ratio, high carrier capacity, high chemical reactivity and biological activity, and tunable size for wide range of beneficial applications [3]. For example, Al₂O₃ nanostructured materials showed remarkable applications such as surface passivation, wear protection, ant-reflection coating, gas diffusion barrier, and catalyst. This is due to good optical properties, high corrosion resistance, surface catalysis, thermal stability, and high surface area of the Al₂O₃ NSs [4, 5]. Aluminium oxide (Al₂O₃) is an inorganic chemical compound of aluminum and oxygen and is commonly referred to as alumina. It is also called corundum due to the crystalline form of aluminum oxide, in which six oxygen atoms surround one

aluminum atom, resulting in porous structures [6]. Al₂O₃ is a light white powder that can be found in amorphous and polycrystalline forms. Al₂O₃ has a melting point of around 2020°C; it is insoluble in water and organic materials but somewhat soluble in acids and alkalis. It is an excellent material with high chemical resistance and thermal stability [4, 6].

Recently, different techniques were used to produce aluminum oxide NSs, from those methods, HWT is a simple, a one-step, scalable, low fabrication temperatures (<100°C), and cost-effective process for preparing metal oxide nanostructures on the surface of their metals [6, 7]. The HWT process involves immersing the metal foils in hot deionized water without any chemical additives [8]. Since nanoparticle size and surface morphology are strongly correlated with the optical, mechanical, and electrical properties, the successful synthesis of the Al₂O₃ nanostructures and studying the growth parameters are very important because they will provide useful information that might help to improve their application performance. In this study, the effect of growth time on the structure and morphology of the aluminum oxide nanostructures was investigated thoroughly by scanning electron microscopy and X-ray diffraction measurement.

2. EXPERIMENTAL PROCEDURE

Hot water treatment (HWT) method was used to prepare Al_2O_3 nanostructures by immersing the aluminum plate (99.99% purity) 1.5 cm×2 cm in hot (75°C) deionized water (DI). First, the samples were prepared using conventional polishing techniques (4000 grit papers). The aluminum metal foils were cleaned in an ultrasonic bath using acetone and then subsequently rinsed with deionized water to remove any surface impurities and dried with an air gun. Al foils were placed in DI water at 75°C for different growth times: 1 min, 7 min, 15, and 30 min as shown in Figure 1. After that, the treatment samples were dried for 6 hours in air. X-ray diffraction (XRD) and scanning electron microscopy (SEM) are used to characterize the structural and morphological properties of the prepared samples.

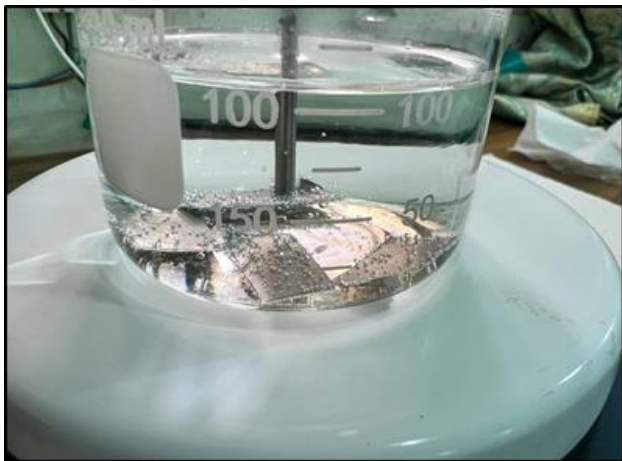


Figure 1. Al foils treated in hot water treatment at 75°C for 7 minutes, 15 minutes, and 30 minutes

3. RESULTS AND DISCUSSION

3.1 Morphological and structural characterization

Figure 2 shows the X-ray diffraction patterns of the (a) aluminum metal foils and treated aluminum metal foils in hot water at 75°C temperatures for different durations (b) 1 minute, (c) 7 minutes, (d) 15 minutes, and (e) 30 minutes.

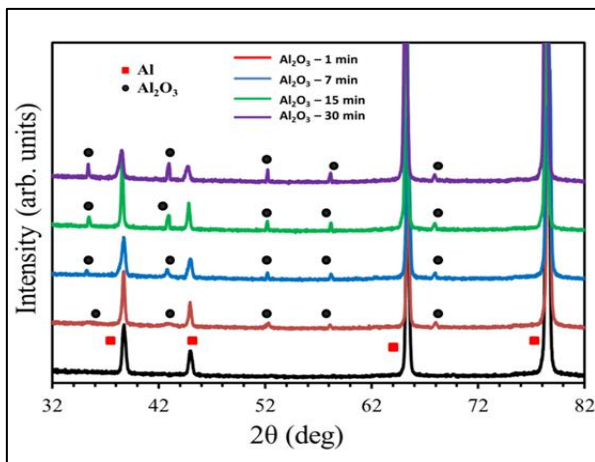


Figure 2. XRD spectra of Al metal substrate, $\alpha\text{-Al}_2\text{O}_3$ nanostructures prepared by HWT at 1 minute, 7 minutes, 15 minutes, and 30 minutes

The XRD pattern for Al metal substrate shows intense peaks located at $2\theta = 38.70^\circ, 44.94^\circ, 65.25^\circ, 78.41^\circ$ which are attributed to the Al (111), (200), (220), and (311) plans respectively. These observations are similar to those published by [9-11]. The obtained peaks were compared with typical diffraction data to identified $\alpha\text{-Al}_2\text{O}_3$ NSs. As shown in Figure 1, there are five recorded diffraction peaks corresponding to (104), (113), (024), (116), (214). These observations are matched well the same structure reported in [9, 12-14]. These standard data are attributed to the rhombohedral structure [15]. Also, XRD results showed that the intensity of the peaks increased when the depositing time increased from 1 min to 30 min and became sharper, this is due to decreasing the crystallite size [14].

The XRD experimental results revealed that the diffraction intensity increases with increasing the hot water treatment time from 1 to 30 min. The sharp and high-intensity peaks suggested an increase in grain size and improved crystallinity and surface texture of nanostructures [16].

The mean crystallite size of $\alpha\text{-Al}_2\text{O}_3$ calculated from the full width at half-maximum (FWHM) of the XRD peak β (in rad), X-ray radiation wavelength used ($\lambda = 1.54060\text{\AA}$), Scherrer constant ($K = 0.9$), and the diffraction angle θ , using Scherrer equation ($D = K\lambda/\beta \cos\theta$) [15]. The calculated average crystalline grain size of $\alpha\text{-Al}_2\text{O}_3$ for the most intense peaks are summarized in the Table 1. From Table 1, it is observed that the crystallite size increases with increasing treatment time due to the grain coalescence with increasing growth rate [7, 14].

Table 1. Average crystal size of $\alpha\text{-Al}_2\text{O}_3$ nanostructures for different HWT times

HWT Time	$2\theta^\circ$ (113)	FWHM (β) Deg	Average Crystal Size (nm)
1 minute	42.90	0.72	11.85
7 minutes	42.80	0.30	28.43
15 minutes	42.90	0.25	34.13
30 minutes	42.90	0.24	35.6

The morphological characteristics of the as-grown Al_2O_3 nanostructures were investigated using scanning electron microscopy (Thermo Scientific™ Quattro SEM). Figure 3 shows SEM images of Al_2O_3 structures grown on Al metal substrate at 75°C for 1, 7, 15, and 30 minutes.

From Figure 3, Al_2O_3 nanostructures are formed after one minute treatment of the Al metal substrates with average nanoparticles size about 66 nm. With increasing treatment time to 7 minutes, overlapped, highly porous (macroporous alumina) nanostructures with an average particle size about 55 nm are observed [17]. Also, as we can see from Figure 2, after 15 minutes of HWT, the density of NSs significantly increased due to high aggregated Al_2O_3 nanoparticles with average size about 42 nm. A uniform distribution of 3D aluminum oxide NSs with average particles size about 40 nm was achieved after 30 minutes. All the sample structures of the alumina particles shown in Figure 2 look like a porous network. The reason for this is that the individual alumina particles with high activity and high surface energy tend to stick with each other to form agglomerates as a neck-formation [17, 18]. These results are in good agreement with previous reported studies [19, 20]. Also, it can notice that the porosity increased with increasing treatment time due to the nanoparticle's agglomeration.

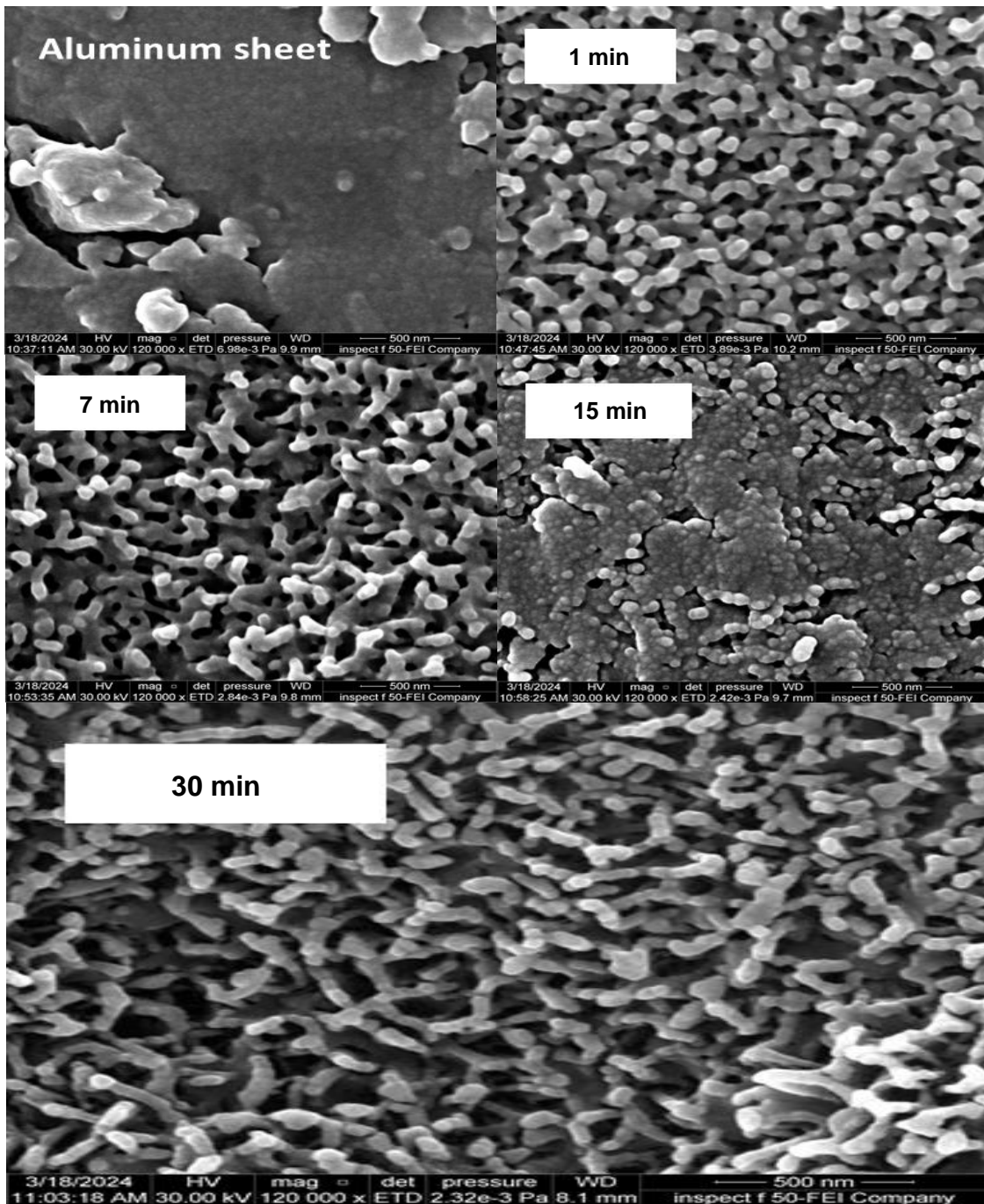


Figure 3. Surface morphology images of the Al metal sheet treated in hot deionized water with various time

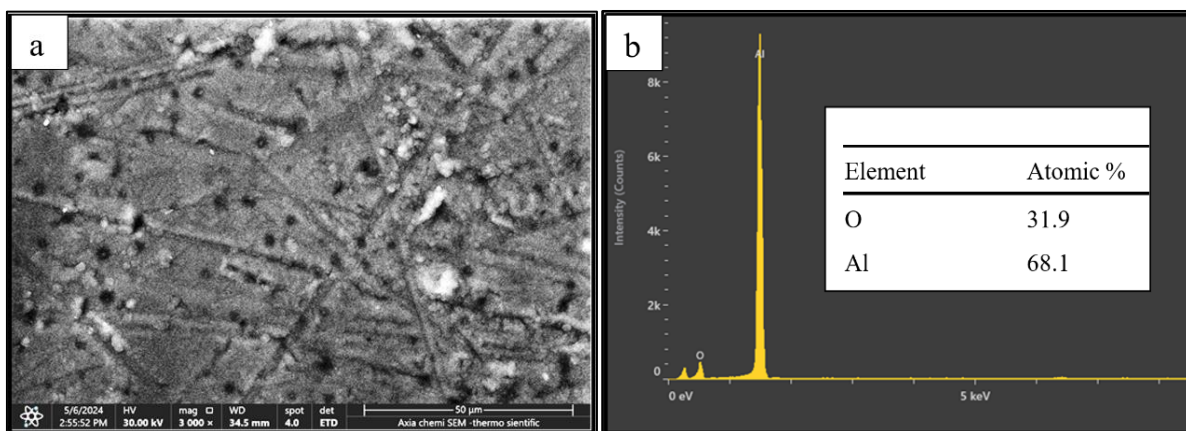


Figure 4. (a) Scanning Electron Microscopy (SEM) image; (b) EDS analysis data for Al metal sheet treated in hot deionized water for 15 minutes

The chemical compositions of the aluminum oxide sample which formed on Al metal sheets surface after HWT at 75°C for 30 minutes were determined by Energy Dispersive Spectroscopy (EDS) and shown in Figures 4(a) and (b). Spectrum analysis Figure 4(b) reveals that the weight percentages of aluminum and oxygen elements were 32 and 68 atomic after hot water treatment for 15 minutes.

3.2 Optical characterization

The optical properties of porous α - Al_2O_3 nanostructures on Al metal substrates were carried out using UV-Vis spectrometer. The measurements have been taken in the wavelength range 200-1000 nm. Figure 5 displays the optical absorbance vs. wavelength spectra of α - Al_2O_3 NSs obtained from surface hot water treatment at various times. Results revealed that Al_2O_3 samples exhibited a strong absorption near 292, 290, 290, and 290 nm at 1, 7, 15, and 30 minutes, respectively. The absorption peaks intensity increased with increasing Al_2O_3 NSs synthesized time in hot de-ionized water due to increasing the oxidation rate of aluminum surface atoms [21, 22]. This means more atoms of aluminum metal are converted to its oxide (alumina) with nonporous and transparent structures.

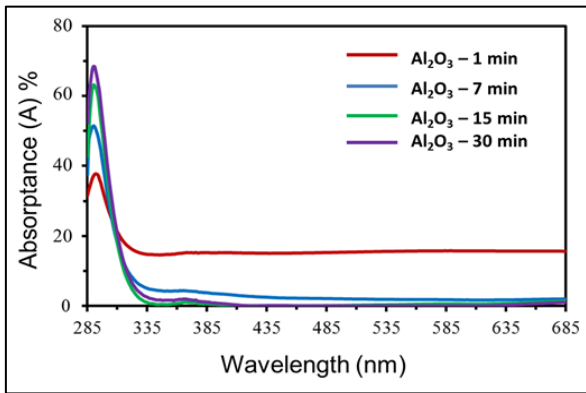


Figure 5. UV-Vis spectra of as-prepared Al_2O_3 nanostructures synthesized at varied synthesis times

Figure 6 displays the absorption coefficient values of NSs at different synthesis times (1, 7, 15, and 30) min that can be estimated from the absorbance (A) and thickness (d) using this relation $\alpha = (2.303 A/d)$ [23, 24]. The extinction coefficient values of Al_2O_3 NSs synthesized at 1, 7, 15, and 30 min that were obtained from the equation ($k = \alpha \frac{\lambda}{4 \times 3.14}$) [28] are presented in Figure 7.

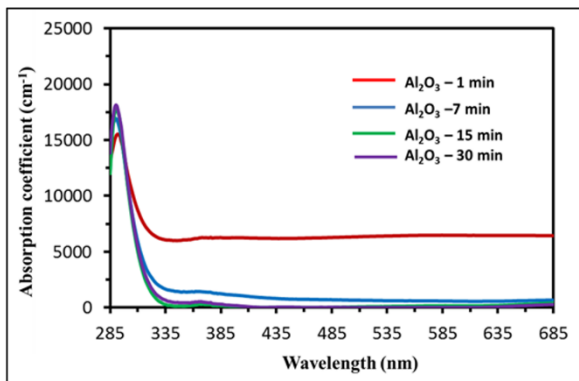


Figure 6. The absorption coefficient of as-prepared Al_2O_3 nanostructures synthesized at varied synthesis times

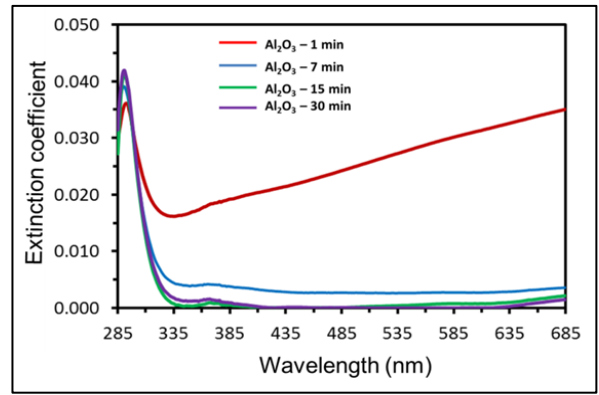
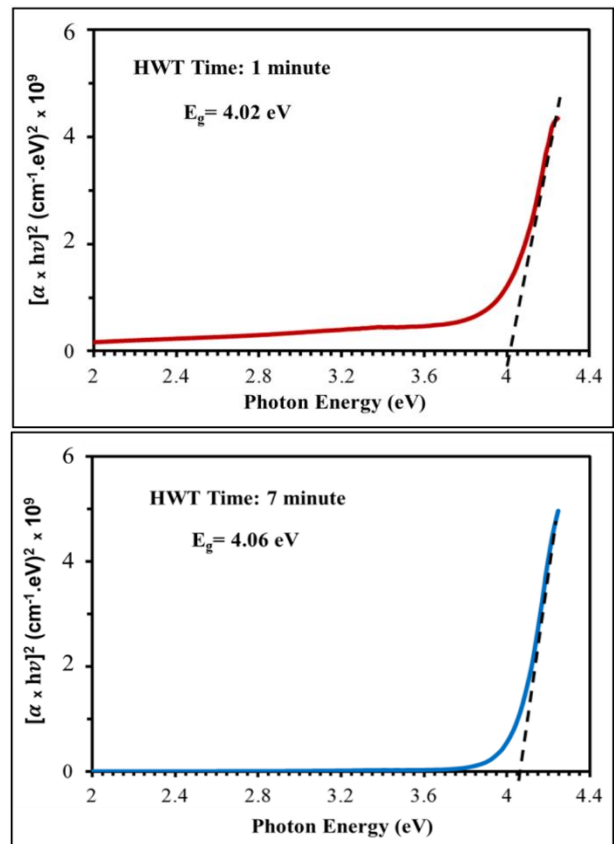


Figure 7. Extinction coefficient of Al_2O_3 NSs synthesized at varied synthesis times

A graph in Figure 8 was drawn between $\log(\alpha h\nu)$ and $\log(h\nu)$ of Al_2O_3 nanostructures for all synthesized samples. The optical band gaps E_g were calculated from photon energy ($h\nu$) using the Tauc's equation [25, 26]:

$$\alpha h\nu = A(h\nu - E_g)^n$$

where, A is a proportionality constant, α is the absorption coefficient. n is the exponent factor that characterizes the nature of electronic transition causing the absorption and can take the values 1/2 and 2, which corresponds to direct or indirect transition, respectively [27]. As shown in Figure 8, the observed results clearly indicated that there is decrease in the band gap values with varying hot water treatment times. The band gaps of aluminum oxide NSs were found to be 4.02 eV, 4.06 eV, 4.05 eV, 4.047 eV for 1 min, 7 min, 15min, and 30 min respectively. The lower band gap of the pores Al_2O_3 NSs may be indicated enhanced oxidation, due defect states, and depending on the shape, size of the nanoparticles [28, 29].



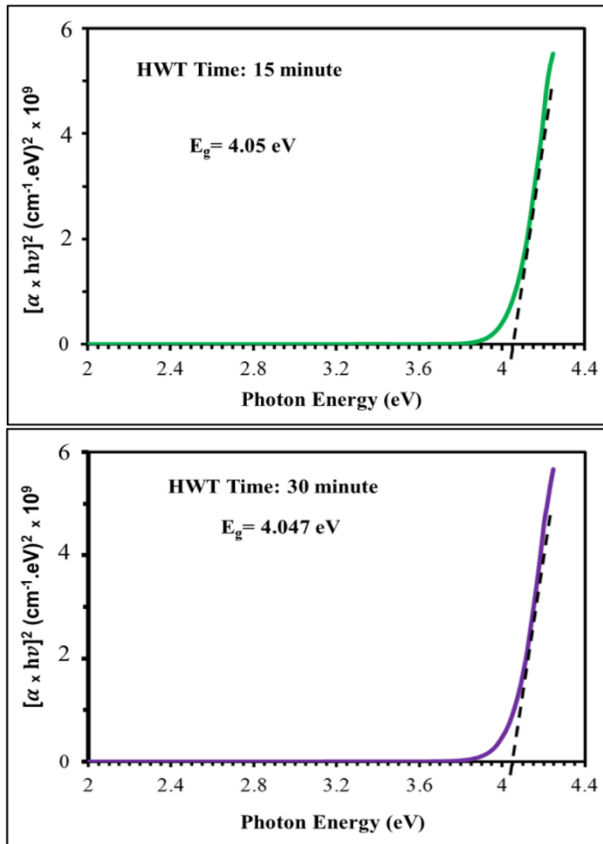


Figure 8. The $[\alpha hv]^2$ versus $h\nu$ plots (using Tauc's equation) Al_2O_3 NSs with different deposition time

4. CONCLUSIONS

In conclusion, a simple and low cost HWT method was used to synthesized aluminum oxide nanostructures on Al metal substrate at low temperature and deferent fabrication times. The obtained surface morphology properties confirm the successful growth and formation of Al_2O_3 nanostructures. Effects of time on the nanostructure growth rate have also been studied. Variation in the HWT treatment time of Al sheets led to the formation of nanostructured semiconducting/metal (Al_2O_3/Al) surfaces. we noticed the nanostructures forming at a faster rate. The formation alumina nanostructured materials took one minute and developed in 7 minutes [20]. This study indicated that the immersion time of Al foils in hot deionized water has a significant effect on the morphology and pore size of alumina. Al_2O_3 samples showed direct band gaps of about 4.04eV, 4.06eV, 4.05eV, and 4.047eV for 1 min, 7 min, 15 min, and 30 min, respectively. The Al_2O_3/Al and nanostructured semiconducting materials prepared in this study could be useful for a wide range of applications, such as solar cells, sensors, optoelectronic devices, catalysis, adsorption, and electronic devices or biomaterials, due to their adjustable pore structure, large surface area, and porous structures.

ACKNOWLEDGMENTS

The authors would like to acknowledge the staff of the Physics Department at the Faculty of Education for Women, University of Kufa, for their support of this research. Additionally, the authors extend their gratitude to Dr. Adel H.

Omran Alkhayatt from the Physics Department at the Faculty of Science, University of Kufa, for his assistance with UV-Vis analysis.

REFERENCES

- [1] Jeevanandam, J., Barhoum, A., Chan, Y.S., Dufresne, A., Danquah, M.K. (2018). Review on nanoparticles and nanostructured materials: History, sources, toxicity and regulations. *Beilstein Journal of Nanotechnology*, 9(1): 1050-1074. <https://doi.org/10.3762/bjnano.9.98>
- [2] Ossai, C.I., Raghavan, N. (2018). Nanostructure and nanomaterial characterization, growth mechanisms, and applications. *Nanotechnology Reviews*, 7(2): 209-231. <https://doi.org/10.1515/ntrev-2017-0156>
- [3] Soltaninejad, H., Zare-Zardini, H., Hamidieh, A.A., Sobhan, M.R., Saeed-Banadaky, S.H., Amirkhani, M.A., Tolueinia, B., Mehregan, M., Mirakhor, M., Eshaghi, F. S. (2020). Evaluating the toxicity and histological effects of Al_2O_3 nanoparticles on bone tissue in animal model: A case-control study. *Journal of Toxicology*, 2020(1): 8870530, <https://doi.org/10.1155/2020/8870530>
- [4] Ahmed, M.I., Jahin, H.S., Dessouki, H.A., Nassar, M.Y. (2021). Synthesis and characterization of $\gamma-Al_2O_3$ and $\alpha-Al_2O_3$ nanoparticles using a facile, inexpensive auto-combustion approach. *Egyptian Journal of Chemistry*, 64(5): 2509-2515. <https://doi.org/10.21608/ejchem.2021.61793.3330>
- [5] Ismail, R.A., Zaidan, S.A., Kadhim, R.M. (2017). Preparation and characterization of aluminum oxide nanoparticles by laser ablation in liquid as passivating and anti-reflection coating for silicon photodiodes. *Applied Nanoscience*, 7: 477-487. <https://doi.org/10.1007/s13204-017-0580-0>
- [6] Shur, V.Y., Mingaliev, E.A., Makaev, A.V., Chezganov, D.S., Kozheletova, I.Y., Pryakhina, V.I. (2019). Creation of nanoparticles and surface nanostructures of alumina by hot water treatment. In *IOP Conference Series: Materials Science and Engineering*, 699(1): 012051. <https://doi.org/10.1088/1757-899X/699/1/012051>
- [7] Saadi, N., Alotaibi, K., Hassan, L., Smith, Q., Watanabe, F., Khan, A.A., Karabacak, T. (2021). Enhancing the antibacterial efficacy of aluminum foil by nanostructuring its surface using hot water treatment. *Nanotechnology*, 32(32): 325103. <https://doi.org/10.1088/1361-6528/abfd59>
- [8] Smith, Q., Burnett, K., Saadi, N., Alotaibi, K., Rahman, A., Al-Mayalee, K., Nawab, A., Khan, A.A., Karabacak, T. (2021). Nanostructured antibacterial aluminum foil produced by hot water treatment against E. coli in meat. *MRS Advances*, 6: 695-700. <https://doi.org/10.1557/s43580-021-00112-2>
- [9] López-Juárez, R., Razo-Perez, N., Pérez-Juache, T., Hernandez-Cristobal, O., Reyes-López, S.Y. (2018). Synthesis of $\alpha-Al_2O_3$ from aluminum cans by wet-chemical methods. *Results in Physics*, 11, 1075-1079, <https://doi.org/10.1016/j.rinp.2018.11.037>
- [10] Ayieko, C.O., Musembi, R.J., Ogacho, A.A., Aduda, B.O., Muthoka, B.M., Jain, P.K. (2015). Controlled texturing of aluminum sheet for solar energy applications. *Advances in Materials Physics and Chemistry*, 5(11):458-466. <https://doi.org/10.4236/ampc.2015.511046>

- [11] Rashad, M., Pan, F., Tang, A., Asif, M. (2014). Effect of graphene nanoplatelets addition on mechanical properties of pure aluminum using a semi-powder method. *Progress in Natural Science: Materials International*, 24(2): 101-108. <https://doi.org/10.1016/j.pnsc.2014.03.012>
- [12] Bharthasaradhi, R., Nehru, L.C. (2015). Preparation and characterisation of nanoscale α -Al₂O₃ by precipitation method. In *AIP Conference Proceedings*, 1665(1): 050141. <https://doi.org/10.1063/1.4917782>
- [13] Oleiwi, H.F., Al-Taay, H.F., Al-Ani, S.K., Tahir, K.J. (2019). Structural and optical properties of Al₂O₃ nanocrystalline: Effect of deposition time. In *AIP Conference Proceedings*, 2144(1): 030027. <https://doi.org/10.1063/1.5123097>
- [14] Bharthasaradhi, R., Nehru, L.C. (2016). Structural and phase transition of α -Al₂O₃ powders obtained by co-precipitation method. *Phase Transitions*, 89(1): 77-83. <https://doi.org/10.1080/01411594.2015.1072628>
- [15] Kim, H.S., Park, N.K., Lee, T.J., Um, M.H., Kang, M. (2012). Preparation of nanosized α -Al₂O₃ particles using a microwave pretreatment at mild temperature. *Advances in Materials Science and Engineering*, 2012(1): 920105. <https://doi.org/10.1155/2012/920105>
- [16] Kadhim, K.R., Mohammed, R.Y. (2022). Effect of annealing time on structure, morphology, and optical properties of nanostructured CdO thin films prepared by CBD technique. *Crystals*, 12(9): 1315. <https://doi.org/10.3390/cryst12091315>
- [17] Xie, Y., Kocaefe, D., Kocaefe, Y., Cheng, J., Liu, W. (2016). The effect of novel synthetic methods and parameters control on morphology of nano-alumina particles. *Nanoscale Research Letters*, 11: 1-11. <https://doi.org/10.1186/s11671-016-1472-z>
- [18] Reichel, F., Jeurgens, L.P.H., Richter, G., Mittemeijer, E.J. (2008). Amorphous versus crystalline state for ultrathin Al₂O₃ overgrowths on Al substrates. *Journal of Applied Physics*, 103(9): 093515. <https://doi.org/10.1063/1.2913505>
- [19] Su, X., Chen, S., Zhou, Z. (2012). Synthesis and characterization of monodisperse porous α -Al₂O₃ nanoparticles. *Applied Surface Science*, 258(15): 5712-5715. <https://doi.org/10.1016/j.apsusc.2012.02.067>
- [20] Ma, P., Jia, Y., Gokuldoss, P.K., Yu, Z., Yang, S., Zhao, J., Li, C. (2017). Effect of Al₂O₃ nanoparticles as reinforcement on the tensile behavior of Al-12Si composites. *Metals*, 7(9): 359. <https://doi.org/10.3390/met7090359>
- [21] Saadi, N.S., Hassan, L.B., Karabacak, T. (2017). Metal oxide nanostructures by a simple hot water treatment. *Scientific Reports*, 7(1): 7158. <https://doi.org/10.1038/s41598-017-07783-8>
- [22] Khedir, K.R., Saifaldeen, Z.S., Demirkan, T., Abdulrahman, R.B., Karabacak, T. (2017). Growth of zinc oxide nanorod and nanoflower structures by facile treatment of zinc thin films in boiling de-ionized water. *Journal of Nanoscience and Nanotechnology*, 17(7): 4842-4850. <https://doi.org/10.1166/jnn.2017.13432>
- [23] Welegergs, G. G., Akoba., R., Sacky, J., Nuru, Z.Y. (2021). Structural and optical properties of copper oxide (CuO) nanocoatings as selective solar absorber. *Materials Today: Proceedings*, 36: 509-513. <https://doi.org/10.1016/j.matpr.2020.05.298>
- [24] Dahrul, M., Alatas, H. (2016). Preparation and optical properties study of CuO thin film as applied solar cell on LAPAN-IPB Satellite. *Procedia Environmental Sciences*, 33: 661-667. <https://doi.org/10.1016/j.proenv.2016.03.121>
- [25] Mallick, P., Sahu, S. (2012). Structure, microstructure and optical absorption analysis of CuO nanoparticles synthesized by sol-gel route. *Nanoscience and Nanotechnology*, 2(3): 71-74. <http://article.sapub.org/10.5923.j.nn.20120203.05.html>
- [26] Tran, T.H., Nguyen, V.T. (2014). Copper oxide nanomaterials prepared by solution methods, some properties, and potential applications: A brief review. *International Scholarly Research Notices*, 2014(1): 856592. <https://doi.org/10.1155/2014/856592>
- [27] Sabbaghan, M., Shahvelayati, A.S., Madankar, K. (2015). CuO nanostructures: Optical properties and morphology control by pyridinium-based ionic liquids. *Spectrochimica Acta Part A: Molecular and Biomolecular Spectroscopy*, 135: 662-668. <https://doi.org/10.1016/j.saa.2014.07.097>
- [28] Johan, M.R., Suan, M.S. M., Hawari, N.L., Ching, H.A. (2011). Annealing effects on the properties of copper oxide thin films prepared by chemical deposition. *International Journal of Electrochemical Science*, 6(12): 6094-6104. [https://doi.org/10.1016/S1452-3981\(23\)19665-9](https://doi.org/10.1016/S1452-3981(23)19665-9)
- [29] Alqadasy, S.S., Chishty, S.Q., Al-Arique, H.Q., Al-Aghbari, E.S., Al-Areqi, N.A., Taiz, Y. (2023) Synthesis and study the structure, morphological and optical properties for TiO₂-Al₂O₃-La₂O₃ prepared by chemical bath deposition. *International Journal of Innovative Science and Research Technology*, pp. 9-15. <https://www.researchgate.net/publication/372189486>